2026 IEEE/SICE International Symposium on System Integration (SII)
January 11-14, 2026. Cancún, México

Toward Robot-Assisted Classification and Selective Picking of *V. harveyi* and Soil Bacteria via Motility Analysis of Inverted Microscope Videos Using XGBoost

Yuki Fujita[1], Sarthak Pathak[2], Alessandro Moro[3],
Yuki Nagase[4], Hiroaki Suzuki[5], Keiichiro Koiwai[6] and Kazunori Umeda[5]

Abstract— **This study proposes a method for accurately estimating the mixing ratio of *V. harveyi* and soil bacteria by analyzing motility in inverted microscope videos and extracting 24 features. Using an XGBoost model, the proposed method outperformed SVM and 1D-CNN approaches. The proposed analytical method will be implemented into a MD-based screening system integrating an inverted microscope, automated stage, and robotic micromanipulator to enable real-time automated classification, selection, and retrieval of antagonistic bacteria during microscopic observation.**

I. INTRODUCTION

In recent years, the global demand for food has been rapidly expanding due to population growth and changes in dietary habits. According to estimates by the Food and Agriculture Organization (FAO) of the United Nations, the world population is expected to reach approximately 9.3 billion by 2050, requiring an increase of about 60% in food production to meet demand [1]. However, terrestrial livestock production faces sustainability challenges, including greenhouse gas emissions and excessive consumption of virtual water, while marine resources are under pressure from overfishing and environmental fluctuations. Against this backdrop, aquaculture has attracted attention as a vital means of ensuring future food security. Nevertheless, aquaculture systems are highly vulnerable to infectious diseases caused by pathogenic bacteria, and the risk of emerging pathogens is further exacerbated by climate change. To address this challenge, robot-assisted microscopic analysis and automated cell manipulation technologies capable of rapid detection and selection of antagonistic bacteria are being increasingly recognized as promising solutions. *V. harveyi* are widely distributed in marine environments and represent a major pathogenic threat to farmed aquatic products. Conversely, certain environmental bacteria may possess antagonistic activity that suppresses the growth of pathogenic bacteria. In recent years, microdroplet (MD)-based cell interaction assays have garnered attention for bacterial screening, enabling the evaluation of metabolic activity and antagonistic effects through co-culture in closed MDs. However, conventional methods have difficulty in individually handling and selectively isolating MDs, and fluorescence labeling of pathogens requires genetic manipulation, which is not applicable to all bacterial species. In the study by Murakami et al. [2], open-type cell array devices with external access were developed, enabling integrated microscopic observation, cultivation, and selective picking. Furthermore, integrating these devices with robotic manipulators and automated stages has the potential to enable fully automated, real-time cell classification, selection, and retrieval based on image analysis results.

Currently, we are developing a cell-interaction based screening system using MDs immobilized on a planar substrate. In this system, *V. harveyi* and environmental bacteria are co-cultured to screen possible antagonistic strain. Here, we found that *V. harveyi* is highly motile compared to environmental bacteria. In this study, we develop an image-based analytical workflow to predict the ratio of *V. harveyi* within the mixed bacterial population. Multiple motility features of bacteria in the videos were extracted, and the mixing ratios were estimated with high accuracy using XGBoost (Extreme Gradient Boosting) [3], a gradient boosting decision tree algorithm. In the future, the proposed analytical method will be implemented into a MD-based screening system integrating an inverted microscope, automated stage, and robotic micromanipulator to enable real-time automated classification, selection, and retrieval of antagonistic bacteria during microscopic observation. By combining consistent image analysis with robotic manipulation control, the system aims to achieve rapid pathogen control in aquaculture and efficient strain acquisition in research environments.

II. RELATED WORKS

Recent advancements in robotic technologies have facilitated the automation of cell and microorganism detection, selection, and retrieval within integrated microscopic systems. Wang et al. [4] developed a microfluidic robot that seamlessly combines a microfluidic device with a high-precision robotic manipulator, enabling automated detection, spatial localization, and aspiration-based retrieval of target

[1]Yuki Fujita is with Precision Engineering Course, Graduate School of Science and Engineering, Chuo University, 1-13-27 Kasuga, Bunkyo-ku, Tokyo, Japan. (Corresponding author: fujita@sensor.mech.chuo-u.ac.jp

[2]Sarthak Pathak is with the College of Engineering, Shibaura Institute of Technology, Tokyo, Japan.

[3]RITECS Inc., 3-5-11 Shibasaki, Tachikawa-shi, Tokyo, Japan.

[4]Yuki Nagase is with Precision Engineering Course, Graduate School of Science and Engineering, Chuo University, Tokyo, Japan.

[5]Hiroaki Suzuki and Kazunori Umeda are with Department of Precision Mechanics, Faculty of Science and Engineering, Chuo University, Tokyo, Japan.

[6]Keiichiro Koiwai is with Laboratory of Genome Science, Tokyo University of Marine Science and Technology, Tokyo, Japan.

978-1-6654-5784-2/26/$31.00 ©2026 IEEE

cells derived from microscopic image analysis. This integration achieves single-cell-level precision, significantly reducing manual intervention while enhancing reproducibility and throughput in large-scale cell screening and functional characterization. Importantly, their work demonstrates the feasibility of real-time coupling between microfluidic chip–based cell handling and robotic arm control, thereby automating micromanipulation tasks that were previously dependent on skilled operators.

Rolda et al. [5] proposed a deep learning–driven automated micromanipulation platform in which high-accuracy target cell detection within microscopic images is directly linked to robotic arm control for selective retrieval. By tightly coupling deep convolutional neural network–based recognition algorithms with robotic actuation, the system achieves robustness against imaging noise and morphological heterogeneity, while also improving operational speed. Their approach further benefits from iterative optimization of recognition accuracy through curated training datasets, as well as from refined motion planning algorithms for the robotic manipulator, leading to a notable increase in successful retrieval rates.

Collectively, these prior studies underscore the effectiveness of integrating microscopy, computer vision, and robotic manipulation to enhance both the efficiency and precision of microbial screening and cell selection workflows. Building upon this foundation, the present study introduces a motility–based analytical framework for estimating the composition ratio of *V. harveyi* and soil bacteria in inverted microscope videos. This framework is ultimately intended for integration into a robotic platform comprising a microscope, automated stage, and micromanipulator, with the goal of enabling real-time, fully automated classification, selection, and retrieval of antagonistic bacteria. Such a system is expected to contribute to rapid pathogen control in aquaculture and to enhance efficiency in research-oriented strain acquisition.

III. PROPOSED METHOD

A. Overview of the Proposed Method

This study proposes a classification framework for estimating the mixing ratio of *V. harveyi* and soil bacteria from microscopic motion, without the need for segmentation or tracking of individual cells. The overall workflow comprises three primary stages: (1) acquisition of bacterial motion videos using an inverted microscope, (2) processing of the recorded video sequences to extract motion features, and (3) classification using an XGBoost [3] model trained on the extracted features. The proposed approach operates without fluorescent labeling or complex preprocessing, thereby enhancing its suitability for future integration into automated systems capable of real-time bacterial classification and selective picking in both aquaculture and research environments.

B. Video Acquisition and Dataset Preparation

Bacterial motion videos were acquired using an inverted microscope under controlled laboratory conditions. The mixing ratio of *V. harveyi* to soil bacteria was systematically varied from 10:0 to 0:10 in increments of 0.5, yielding a total of 21 distinct mixture conditions. For each condition, videos were recorded at a frame rate of 9 frames per second (fps), with a total of 27 frames per video, at a spatial resolution of 1920×1200 pixels. To ensure spatial diversity in bacterial distribution, each condition is recorded ten times while varying the observation position across the sample.

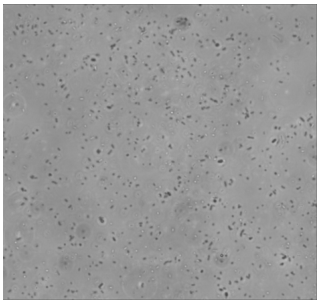

Fig. 1: Original image with a mixing ratio of 5:5

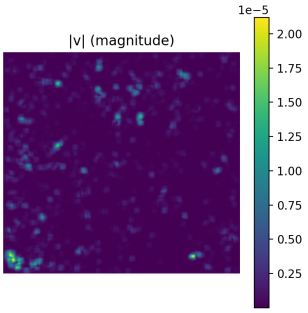

Fig. 2: Magnitude of the velocity vector for each pixel at a mixing ratio of 5:5

C. Motion Feature Extraction

Each acquired video was spatially partitioned by cropping the original 1920×1200-pixel frame into six regions of 640×600 pixels, as illustrated in Fig. 1. This partitioning enables localized motion analysis and effectively increases the number of samples for training.

Dense optical flow was computed using the Farnebäck method [6], which estimates pixel-wise motion vectors between consecutive frames based on local polynomial approximations of image intensity. This approach provides smooth and robust flow fields across different spatial scales, making it suitable for analyzing subtle bacterial movements without explicit cell segmentation or tracking.

From each optical flow field, 24 statistical and structural features were extracted and grouped into six categories: (1) velocity statistics, (2) directional statistics, (3) motion diversity indices, (4) frequency-domain features, (5) spatial gradient energy indices, and (6) local motion pattern indices. These features comprehensively represent motion magnitude, directionality, heterogeneity, and local collective behaviors observed in bacterial populations.

All features were standardized to zero mean and unit variance before classification. For each mixture condition, 50 samples were used for training, and the remainder were reserved for validation and testing.

1) Velocity Statistics: Velocity statistics provide fundamental measures of bacterial motility and its spatial distribution. In this study, we compute the mean, standard deviation, and median of the optical flow vector magnitudes, as well as the mean velocities for the top 25%, 10%, 5%, and 1% of pixels ranked by magnitude. These indicators allow detection of locally high-mobility regions even when the overall motion is small, as shown in Fig. 2.

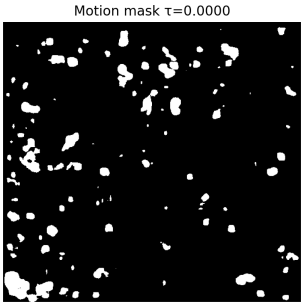

Fig. 3: Mask image of moving pixels with a mixing ratio of 5:5

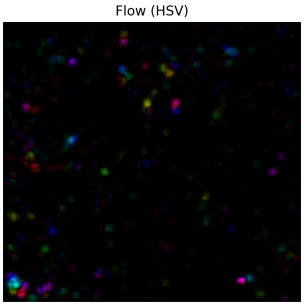

Fig. 4: HSV color visualization chart of direction and magnitude of velocity

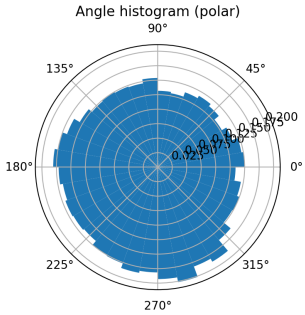

Fig. 5: Polar coordinate histogram of angular distribution for a mixing ratio of 5:5

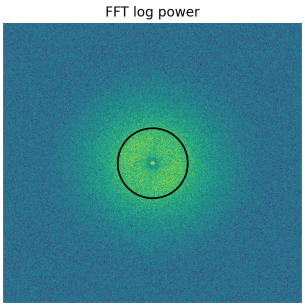

Fig. 6: FFT log power spectrum and cutoff circle of difference images with a mixing ratio of 5:5

To quantify the spatial extent of active motion, we compute the proportion of moving pixels. For each frame t, let m_{ij}^t be the motion magnitude between frames t and $t+1$. A threshold τ^t is defined as:

$$\tau^t = \text{median}(m_{ij}^t) + 1.5 \times \text{MAD}(m_{ij}^t) \tag{1}$$

where MAD denotes the median absolute deviation, a robust measure against outliers.

The proportion r^t of pixels exceeding the threshold is:

$$r^t = \frac{1}{HW} \sum_{i=1}^{H} \sum_{j=1}^{W} \begin{cases} 1, & m_{ij}^t > \tau^t \\ 0, & \text{otherwise} \end{cases} \tag{2}$$

The average proportion across all frames is:

$$\text{Proportion of moving pixels} = \frac{1}{T-1} \sum_{t=1}^{T-1} r^t \tag{3}$$

This metric captures not only motion magnitude but also the spatial prevalence of high-motion pixels, enabling identification of locally active bacterial clusters, as shown in Fig. 3.

2) Directional Statistics: Directional statistics characterize the directional properties of bacterial motion. In this method, the mean and standard deviation of the directional concentration are calculated to assess whether the motion is biased toward a specific direction (directional motion) or random (isotropic motion). High concentration values indicate dominant, ordered movement, while low values indicate complex, multi-directional motion.

3) Motion Diversity Indices: Motion diversity indices quantify the complexity and variability of motion patterns. In this method, the mean and standard deviation of the entropy of the velocity vector directions are calculated. High entropy values indicate diverse directions and velocities, while low entropy values indicate uniform and ordered motion. This allows for the classification of bacterial motion patterns into monotonic and diverse types. Fig. 4 shows an HSV color visualization diagram of direction and magnitude of velocity. Fig. 5 further illustrates the angular distribution in polar coordinates for a mixing ratio of 5:5.

4) Frequency-Domain Features: Frequency-domain features are obtained from the power spectrum of the optical flow magnitude. A Fast Fourier Transform (FFT) is applied, and the ratio of high-frequency power to the total power is calculated. The mean and standard deviation of this ratio across frames are used as features. Higher ratios indicate fine, abrupt motion, while lower ratios indicate smooth, large-scale motion. Fig. 6 shows an FFT log power spectrum of a difference image with the cutoff circle separating low- and high-frequency components.

5) Spatial Gradient and Autocorrelation Indices: This feature category quantifies local intensity variation and spatial continuity within the velocity field. The mean and standard deviation of spatial autocorrelation are computed to measure the similarity of motion patterns between neighboring regions. Higher values indicate predominant continuous motion across space, whereas lower values reflect pronounced local heterogeneity.

6) Local Motion Pattern Indices: Local motion pattern indices characterize the local structural properties of bacterial motion. The mean and standard deviation of divergence are computed to quantify the degree of local contraction or expansion, with positive values indicating spreading motion and negative values indicating converging motion, as shown in Fig. 7.

Similarly, the mean and standard deviation of vorticity are computed to assess the strength and distribution of local rotational motion. Large vorticity values indicate motion involving rotation, whereas small values indicate predominantly linear or diffusive motion, as shown in Fig. 8.

Furthermore, motion regions obtained by thresholding the optical flow field are analyzed via connected component analysis. The number of connected components, the mean and standard deviation of component areas, and the 95 percentile of component area are calculated to quantitatively assess whether bacterial populations are isolated or widely distributed.

D. Model Architecture and Training

In this study, 24 features from six categories, extracted via optical flow analysis, are used as inputs to predict bacterial mixing ratios using XGBoost [3], a gradient boosting decision tree model. XGBoost incrementally constructs an ensemble of decision trees, where each subsequent tree corrects the residuals of the previous ones, enabling accurate modeling of complex non-linear relationships and feature

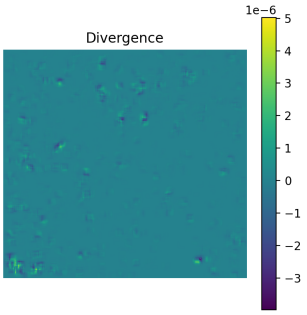

Fig. 7: Divergence map with a mixing ratio of 5:5

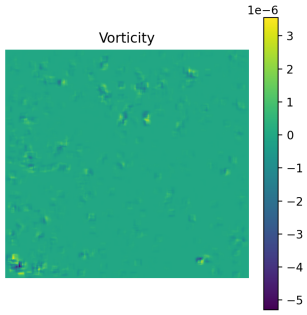

Fig. 8: Vorticity map for a mixing ratio of 5:5

interactions. Owing to the inherent characteristics of tree-based models, no feature scaling or normalization is required, allowing diverse statistical, distributional, and spatial descriptors to be integrated into a unified input space.

The input vector comprises six categories: velocity statistics, directional statistics, motion diversity indices, frequency-domain features, spatial gradient and autocorrelation indices, and local motion pattern indices. Each category represents a distinct aspect of bacterial motility, and their combination provides a high-dimensional representation of complex motion patterns that cannot be characterized by a single metric.

For training, 50 samples per condition are selected from ten recordings taken at different positions. Hyperparameters, including maximum tree depth, learning rate, and number of trees, are optimized via grid search and cross-validation to mitigate overfitting. Model performance is evaluated on an independent test dataset, with accuracy, recall, and F1 score as evaluation metrics.

IV. EXPERIMENTS

A. Overview of the Experiments

In this study, a dataset acquired using an inverted microscope was employed to classify the mixing ratios of *V. harveyi* and soil bacteria. Classification was performed using 24 motion features, and classification accuracy was evaluated. Optimal model hyperparameters were also determined. Furthermore, performance comparisons were conducted with Support Vector Machine (SVM) [7] and lightweight one-dimensional Convolutional Neural Network (1D-CNN) [8] models, as well as between using all features and using only the most important features.

B. Sample Preparation

The *V. harveyi* strain used in this study was kindly provided by Dr. Koiwai. Environmental bacterial strains were isolated from soil samples collected from the flower beds at Chuo University Korakuen Campus and subsequently purified through membrane filtration. Both bacterial strains were stored at $-80\,^{\circ}\mathrm{C}$ until use. For experimental preparation, a small aliquot from each frozen stock was inoculated into growth medium and cultured overnight at $25\,^{\circ}\mathrm{C}$ with shaking. Cell concentrations were then determined, and each bacterial suspension was diluted to a final density of 5×10^8 cell/ml. The two bacterial suspensions were mixed at the desired ratios, placed on glass slides, and mounted as microscope specimens. Observations were conducted using an inverted microscope (Nikon Ti), and videos were recorded with a CCD camera.

C. Dataset

The data were acquired as described in Section III-B, and each video was then cropped into six regions of 640 × 600 pixels, resulting in six stacked images per video and a total of 1,260 samples. From these, 50 samples per condition were randomly selected for model training, and the remaining samples were used as the test dataset.

D. Hyperparameter Settings

In this study, multiple hyperparameters of the XGBoost [3] model were exhaustively explored to identify the configuration that maximized generalization performance. The parameters examined included maximum tree depth (5, 7), learning rate (0.05, 0.1), number of trees (400, 800), subsampling rate (0.8, 1.0), feature subsampling rate (0.8, 1.0), L2 regularization strength (1.0, 3.0), and the minimum sum of instance weight required for child node creation (1.0, 3.0). A five-fold cross-validation was applied to all parameter combinations, and the configuration yielding the highest accuracy was adopted. The optimal setting was found to be 80% feature subsampling, a learning rate of 0.05, maximum tree depth of 5, minimum sum of instance weight of 1.0, 800 trees, and L2 regularization strength of 3.0. This configuration effectively suppressed overfitting while capturing complex feature interactions with high accuracy.

E. Classification of Mixing Ratios Using 24 Features

Using the optimal hyperparameters determined in Section IV-D, the classification of Vibrio and soil bacteria mixing ratios was conducted based on 24 motion features. The classification results are shown in the confusion matrix in Fig. 9. The overall classification accuracy reached 85.7%, indicating that the mixing ratios could be distinguished with comparatively high accuracy. Furthermore, the results showed that classification performance was high under conditions where either *V. harveyi* or soil bacteria predominated, whereas accuracy tended to decline when their mixing ratios were comparable.

Permutation importance analysis results are presented in Fig. 10. As shown, the features contributing most substantially to the predictive performance of the model were *highfreq_ratio_mean* and *mag_p50*. The former represents the mean proportion of high-frequency components, capturing fine-scale fluctuations and rapid directional changes that are characteristic of the highly motile *V. harveyi*, whereas the latter corresponds to the median magnitude of velocity vectors, reflecting the overall motility level and smooth trajectories that are more typical of soil bacteria. This contrast in temporal and spatial motion signatures allows these two features to effectively discriminate between fast,

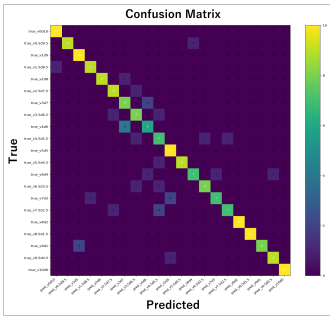

Fig. 9: Classification results using 24 features

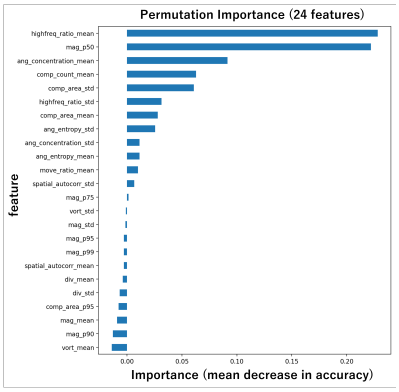

Fig. 10: Permutation importance results using 24 features

irregular swimming patterns and slow, steady movements. The prominence of these features therefore indicates that the model's decision-making process predominantly relies on motion frequency characteristics and representative measures of velocity distribution that embody the fundamental behavioral differences between the two bacterial types.

In addition, features such as *ang_concentration_mean*, *comp_count_mean*, and *comp_area_std* exhibited moderate importance, implying that morphological and spatial attributes—such as the directional concentration of motion, the number of discrete regions, and the variability in their areas—provide supplementary discriminative information that enhances classification performance.

Conversely, features including *mag_p75* and *vort_std* displayed near-zero importance, indicating a negligible contribution within the current model. This outcome suggests that such features may be highly correlated with other variables or offer limited discriminatory capacity for this classification task, rendering them potential candidates for exclusion in future feature selection or model simplification efforts.

Collectively, these findings indicate that the model primarily exploits motion frequency characteristics and velocity distribution as the principal criteria for classification, while morphological and spatial descriptors act as complementary factors. This underscores the efficacy of employing multi-dimensional feature extraction for the quantitative analysis of microbial motility patterns. Furthermore, these results suggest that future feature design should incorporate multi-scale temporal dynamics, frequency-domain descriptors, and measures of trajectory stability or coherence. By capturing both global motion tendencies and localized fluctuations, such features may enhance interpretability and generalization across different bacterial species and environmental conditions.

TABLE I: Classification accuracy of XGBoost, SVM, and 1D-CNN

Model	Accuracy
XGBoost (24 features)	0.857
SVM	0.848
1D-CNN	0.842

TABLE II: Classification accuracy using all features versus only the most important features

Case	Features Used	Accuracy
all_features	All 24 features	0.857
highfreq_only	highfreq_ratio_mean	0.148
mag_p50_only	mag_p50	0.071
both_hf_mag	highfreq_ratio_mean, mag_p50	0.210

F. Comparison with SVM and 1D-CNN

To evaluate the performance of different modeling approaches, we compared the proposed XGBoost classifier with SVM [7] and 1D-CNN [8]. All models were trained using the same 24 motion features extracted from the optical flow sequences. The obtained accuracies were 84.76% for the SVM [7], 84.29% for the 1D-CNN [8], and 85.7% for the proposed XGBoost.

The SVM [7] achieved stable performance, showing that the extracted features provide clear class separability. However, its kernel-based decision boundaries could not fully capture complex nonlinear relationships among motion features. The 1D-CNN [8], while capable of learning local dependencies within the feature vector, showed slightly lower accuracy due to the limited dataset size, which restricted its ability to generalize and avoid overfitting.

In contrast, XGBoost [3] achieved the highest accuracy and exhibited more consistent results across random splits. These findings suggest that gradient-boosting frameworks can effectively model nonlinear feature interactions and maintain robustness in small-scale biological datasets, offering a better balance between accuracy and interpretability than SVM [7] or 1D-CNN [8].

G. Comparison with Using Only the Most Important Features

This section evaluates the classification performance when using only the top-ranked features identified by the Permutation Importance analysis, specifically *highfreq_ratio_mean* and *mag_p50*. Three experimental configurations were examined: (1) using only *highfreq_ratio_mean*, (2) using only *mag_p50*, and (3) using both features in combination. For reference, the classification result obtained using all 24 extracted motion features is also presented. Table II summarizes the results, while Fig. 11 illustrates the confusion matrices for the three reduced-feature configurations.

The results indicate that the exclusive use of the most important features, either individually or in combination,

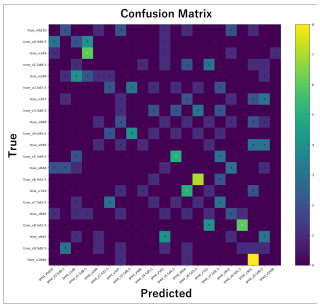

(a) Result using only high-freq_ratio_mean

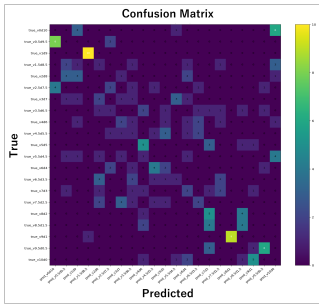

(b) Result using only mag_p50

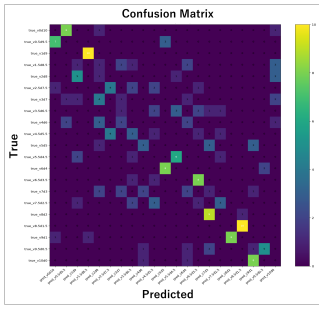

(c) Result using both features

Fig. 11: Results using the most important features

resulted in a substantial decrease in classification accuracy compared to the use of all features. Although *high-freq_ratio_mean* and *mag_p50* were identified as highly influential in the prediction process, they alone do not provide sufficient discriminative capacity to accurately classify the bacterial mixture ratios. Even when both features were used together, the accuracy reached only 0.210, underscoring the necessity of incorporating additional complementary features.

This observation underscores the importance of feature diversity in the proposed method. While frequency-domain characteristics and velocity magnitude distributions constitute key determinants of classification, morphological and spatial descriptors—such as angular concentration, component count, and component area variability—serve a crucial complementary role. Overall, the ablation study demonstrates that reliance on a small subset of features markedly restricts classification performance, thereby reaffirming the necessity of integrating multiple heterogeneous features to achieve robust bacterial mixture ratio estimation.

V. CONCLUSION

In this study, we addressed the classification of mixing ratios between *V. harveyi* and soil bacteria using 24 motion features extracted from bacterial motility videos captured with an inverted microscope. The experimental results demonstrated that employing all features achieved a classification accuracy of 85.7%, confirming the effectiveness of the XGBoost [3] model even under limited-data conditions. Comparative experiments with SVM [7] and 1D-CNN [8] models showed slightly lower performance, mainly because these methods could not effectively model nonlinear feature relationships in a small dataset. Furthermore, the feature importance analysis revealed that the average ratio of high-frequency components and the median magnitude of velocity vectors were the most influential predictors, suggesting that the model primarily leverages frequency-domain motion characteristics and representative velocity metrics as core decision criteria.

Future work aims to integrate the proposed method into a robotic system consisting of an inverted microscope, automated stage, and micromanipulator to enable real-time automated classification and selection of cells and bacteria during microscopic observation. This classification capability will allow the robotic system to selectively pick MDs in which the growth of *V. harveyi* is suppressed after co-culture with environmental bacteria. By combining automated classification with robotic manipulation, the system will facilitate the rapid identification and retrieval of antagonistic strains, contributing to pathogen control in aquaculture and efficient strain acquisition in research environments.

In addition, we plan to extend the current framework to handle more diverse environmental conditions, longer observation durations, and larger datasets to evaluate robustness and scalability. Incorporating regression-based ratio estimation and ordinal evaluation metrics will also enable more continuous and interpretable assessments of bacterial dynamics. These future developments are expected to advance toward a robust, scalable robotic screening platform capable of real-time analysis and selective manipulation in various microscopic environments.

REFERENCES

[1] United Nations, "Feeding the World, Sustainably," United Nations Chronicle, Available online: https://www.un.org/en/chronicle/article/feeding-world-sustainably (accessed 11 August 2025).

[2] T. Murakami, H. Teratani, D. Aoki, M. Noguchi, M. Tsugane, and H. Suzuki, "Single-cell trapping and retrieval in open microfluidics," iScience, vol. 26, no. 11, p. 108323, Nov. 2023.

[3] T. Chen and C. Guestrin, "XGBoost: A Scalable Tree Boosting System," in Proceedings of the 22nd ACM SIGKDD International Conference on Knowledge Discovery and Data Mining, pp. 785–794, Aug. 2016.

[4] Y. Wang et al., "A microfluidic robot for rare cell sorting based on machine vision identification and multi-step sorting strategy," Talanta, vol. 226, p. 122136, May 2021.

[5] A. Da Rold, M. Furiato, A. M. A. Zaki, M. Carnevale, and H. Giberti, "Deep learning-based robotic sorter for flexible production," Procedia Computer Science, vol. 217, pp. 1579–1588, 2023.

[6] G. Farnebäck, "Two-Frame Motion Estimation Based on Polynomial Expansion," in Image Analysis, vol. 2749, J. Bigun and T. Gustavsson, Eds., in Lecture Notes in Computer Science, vol. 2749. , Berlin, Heidelberg: Springer Berlin Heidelberg, pp. 363–370, 2003.

[7] C. Cortes and V. Vapnik, "Support-vector networks," Mach Learn, vol. 20, no. 3, pp. 273–297, Sep. 1995.

[8] S. Kiranyaz, T. Ince, and M. Gabbouj, "Real-Time Patient-Specific ECG Classification by 1-D Convolutional Neural Networks," IEEE Trans. Biomed. Eng., vol. 63, no. 3, pp. 664–675, Mar. 2016.